LONG BASELINE NEUTRINO BEAMS AND APPEARANCE EXPERIMENTS

ANTONIO EREDITATO
INFN Napoli, Complesso Univ. Monte Sant'Angelo
80125 Napoli, Italy
E-mail: Antonio.Ereditato@na.infn.it

PASQUALE MIGLIOZZI
CERN, Geneva, Switzerland and INFN Napoli, Complesso Univ. Monte Sant'Angelo
80125 Napoli, Italy
E-mail: Pasquale.Migliozzi@cern.ch

ABSTRACT

In this paper we review the main characteristics of the future Long Baseline neutrino beams, and their capabilities for appearance experiments searching for $\nu_\mu \leftrightarrow \nu_\tau$ oscillations. General features of τ appearance experiments will be discussed and some of the proposed experiments described.

1. Introduction

If one attributes the apparent deficit of atmospheric muon neutrinos to neutrino oscillations, as measured in the Super-Kamiokande [1)] and Kamiokande [2)] experiments, a small Δm^2 ($\sim 10^{-2} - 10^{-3}$ eV^2) and a large mixing angle ($\sin^2 2\theta > 0.9$) emerge. The result of the reactor experiment CHOOZ [3)], which explored the same parameter region, together with Super-Kamiokande exclude $\nu_\mu \leftrightarrow \nu_e$ oscillations down to the level of 10^{-3} eV^2, so favouring the explanation of the Super-Kamiokande result in terms of $\nu_\mu \leftrightarrow \nu_\tau$ (or more exotically $\nu_\mu \leftrightarrow \nu_{sterile}$) oscillations.

The region of oscillation parameters indicated by the atmospheric neutrino anomaly is hardly accessible by short baseline searches. Long baseline experiments are needed to probe the small Δm^2 region favoured by the existing data. A new generation of experiments with ν_μ beams produced by accelerator is being planned. A neutrino beam has been recently commissioned from KEK to the Super-Kamiokande detector, about 250 km away [4)]. The muon neutrino energy is, however, below the kinematical threshold to produce τ leptons. Only disappearance of ν_μ could be probed.

At Fermilab, the experiment MINOS [5)] is approved and will use the NuMI beam [6)] from Fermilab to the Soudan Mine, at 730 km distance, to test the hypothesis of neutrino oscillations with $\Delta m^2 \sim 10^{-2} - 10^{-3}$ eV^2. Finally, several ideas for long baseline (LBL) experiments [7,8,9,10,11)] have been proposed to use the future NGS beam [12)] from CERN to the Gran Sasso Laboratory, 732 km away from the source.

Both the NuMI and the NGS beams will allow for τ appearance experiments with a sensitivity adequate to confirm of disprove the Super-Kamiokande result with artificially produced neutrinos.

2. Classification of neutrino oscillation experiments

There are two main strategies to search for neutrino oscillations: to perform *disappearance* and *appearance* experiments. In the first case the experimental requirement is a neutrino source with well known intensity. Hence, the sensitivity of disappearance experiments is limited by systematic uncertainties on the knowledge of the neutrino flux intensity. For this reason, the measurement of the flux can profit from another detector placed at a different distance from the source. The latter is called a "near detector". The experiment has to look for (small) deviations of the oscillation probability $P(\nu_\alpha \leftrightarrow \nu_\alpha)$ from 1 (*diagonal test*). Normally, disappearance experiments cannot detect the flux variations for the flavour ν_β due to $\nu_\alpha \leftrightarrow \nu_\beta$ oscillations. They can only look for $\nu_\alpha \leftrightarrow \nu_x$ oscillations (where x can be any neutrino specie.) The experiment can be carried on even if the fraction of ν_β in the beam with respect to the main component ν_α is not negligible.

An experiment searching for $\nu_\alpha \leftrightarrow \nu_\beta$ is defined as an *appearance* experiment if the detector is sensitive to the interactions of ν_β neutrinos. They have to be very efficient in the detection of ν_β. Their sensitivity is, indeed, limited by the uncertainty in the contamination of ν_β to the main ν_α flux.

Appearance experiments can be further subdivided into two classes: *direct appearance* and *indirect appearance* searches. The latter class includes those experiments which are able to separate ν_β induced interactions from background on a statistical basis, either by means of kinematics or by looking at deviation of the cross section ratio of charged over neutral current from expectations. In *direct appearance* experiments neutrino oscillations are detected through the identification of the lepton β, produced in ν_β charged current interactions on an event by event basis.

It is important to note that, since the appearance of a different flavour manifests through the interaction of ν_β with the experimental target, the energy of this neutrino must be high enough to produce its lepton partner. This sets, for a given oscillation search, a lower limit on the neutrino energy. As an example, due to the kinematical threshold to produce a τ lepton of $\sim 3.5\ GeV$, a high-energy beam is needed for $\nu_\mu \leftrightarrow \nu_\tau$ appearance experiments.

In the following, we will briefly review the main features of appearance experiments, focusing on $\nu_\mu \leftrightarrow \nu_\tau$ oscillation searches.

2.1. NC/CC test for $\nu_\mu \leftrightarrow \nu_\tau$ oscillations

We assume to start with a pure ν_μ beam with flux $\phi_\mu(E, x)$. The expected number of charged current (CC) interactions in a detector of length l, placed at a distance L from the source, can be written as

$$n_{cc}(E) = \int_L^{L+l} \phi_\mu(E,x)\sigma_{cc}(E)dx$$

Under the same assumptions, the number of neutral current (NC) interactions is

$$n_{nc}(E) = \int_L^{L+l} \phi_\mu(E,x)\sigma_{nc}(E)dx = \frac{\sigma_{nc}(E)}{\sigma_{cc}(E)} n_{cc}(E)$$

In the absence of neutrino oscillations the total number of interactions is given by

$$N_{cc} = S \int n_{cc}(E)dE \tag{1}$$

$$N_{nc} = S \int n_{nc}(E)dE = \frac{\langle \sigma_{nc} \rangle}{\langle \sigma_{cc} \rangle} N_{cc} \tag{2}$$

S being a normalisation factor. If neutrino oscillations occur, one has to consider that the τ lepton produced in ν_τ CC interactions may decay into a muon. Therefore, if this muon is detected the ν_τ event will be classified as a ν_μ charged current interaction. In addition, the cross section for ν_μ and ν_τ are slightly different ($\sigma_\tau < \sigma_\mu$) and the interaction rate of ν_τ is suppressed by a factor η ($= \sigma_\tau/\sigma_\mu$). Taking into account ν_τ interactions, the expected number of CC events in the presence of neutrino oscillations becomes

$$\begin{aligned} N_{cc}^{osc} &= S \int \{ n_{cc}(E) [1 - P_{\mu\tau}] + n_{cc}(E) P_{\mu\tau} \eta BR_{\tau\mu} \} dE \\ &= S \left\{ \int n_{cc}(E)dE + \int n_{cc}(E)[\eta BR_{\tau\mu} - 1] P_{\mu\tau} dE \right\} \end{aligned} \tag{3}$$

while the number of NC interactions is

$$N_{nc}^{osc} = S \int \left\{ \frac{\sigma_{nc}(E)}{\sigma_{cc}(E)} n_{cc}(E) + n_{cc}(E) P_{\mu\tau} \eta [1 - BR_{\mu\tau}] \right\} dE \tag{4}$$

By using expressions (1), (2), (3) and (4) it is possible to derive the expected NC/CC ratio with or without oscillations

$$r_{nc/cc} = \frac{N_{nc}^{osc}}{N_{cc}^{osc}} = \frac{\int \frac{\sigma_{nc}(E)}{\sigma_{cc}(E)} n_{cc}(E)dE + \int n_{cc}(E) P_{\mu\tau} \eta (1 - BR_{\mu\tau}) dE}{\int n_{cc}(E)dE + \int n_{cc}(E) P_{\mu\tau} (\eta BR_{\mu\tau} - 1) dE} \tag{5}$$

$$R_{nc/cc} = \frac{N_{nc}}{N_{cc}} = \frac{\int \frac{\sigma_{nc}(E)}{\sigma_{cc}(E)} n_{cc}(E)dE}{\int n_{cc}(E)dE} \tag{6}$$

From equations (5) and (6) we obtain that $R_{nc/cc} < r_{nc/cc}$. If the difference $r_{nc/cc} - R_{nc/cc}$ is consistent with zero (no evidence for neutrino oscillations) a region in the parameter plane $\Delta m^2 - \sin^2 2\theta$ may be excluded at a given confidence level. Using equations (5) and (6), one sees that the difference $r_{nc/cc} - R_{nc/cc}$ is positive. Hence a one-sided gaussian distribution can be used to define the 90% C.L. upper-limit on the oscillation probability. One obtains

$$\int \left\{ n_{cc}[(1 - 1.28\sigma_R)\eta(1 - BR_{\mu\tau}) - R_{nc/cc}(\eta BR_{\mu\tau} - 1)]P_{\mu\tau} \right\} dE \leq 1.28\sigma_R N_{cc} \tag{7}$$

In the limit of large $\Delta m^2 (\Delta m^2 \gg E/L)$ equation (7) can be written as

$$\sin^2 2\theta \leq \frac{2 \times 1.28\sigma_R}{[(1 - 1.28\sigma_R)\eta(1 - BR_{\mu\tau}) - R_{nc/cc}(\eta BR_{\mu\tau} - 1)]} \tag{8}$$

The asymptotic value of $\sin^2 2\theta$ only depends on σ_R, namely on the statistical accuracy of the experiment in the measurement of $R_{nc/cc}$. Possible systematical errors must be included in σ_R. For $\sin^2 2\theta = 1$ the asymptotic limit on Δm^2 can be written as

$$\Delta m^2 \leq \sqrt{\frac{\sin^2 2\theta(\Delta m^2 \to \infty)}{2 \times 1.267 \langle \left(\frac{L}{E}\right)^2 \rangle}} \tag{9}$$

2.2. Direct appearance *experiments searching for $\nu_\mu \leftrightarrow \nu_\tau$ oscillations*

We assume to deal with a ν_μ beam with negligible ν_τ contamination. The ratio of the observed ν_τ charged current over ν_μ interactions can be expressed as

$$\begin{aligned}
\frac{N_\tau}{N_\mu} &= \frac{\int \phi_\mu(E)\sigma_\tau P_{\mu\tau}\varepsilon_\tau dE}{\int \phi_\mu(E)\sigma_\mu\varepsilon_\mu BR dE} \\
&= \frac{\int \phi_\mu(E)\sigma_\tau P_{\mu\tau}\varepsilon_\tau BR dE}{\int \phi_\mu(E)P_{\mu\tau}\sigma_\tau dE} \frac{\int \phi_\mu(E)\sigma_\mu dE}{\int \phi_\mu(E)\sigma_\mu\varepsilon_\mu dE} \frac{\int \phi_\mu(E)P_{\mu\tau}\sigma_\tau dE}{\int \phi_\mu(E)\sigma_\mu\varepsilon_\mu dE} \\
&= BR\frac{\langle\varepsilon_\tau\rangle}{\langle\varepsilon_\mu\rangle} \frac{\int \phi_\mu(E)P_{\mu\tau}\sigma_\tau dE}{\int \phi_\mu(E)P_{\mu\tau}dE} \frac{\int \phi_\mu(E)dE}{\int \phi_\mu(E)\sigma_\mu dE} \frac{\int \phi_\mu(E)P_{\mu\tau}dE}{\int \phi_\mu(E)dE} \\
&= BR\frac{\langle\varepsilon_\tau\rangle}{\langle\varepsilon_\mu\rangle} \frac{\langle\sigma_\tau\rangle}{\langle\sigma_\mu\rangle} \langle P_{\mu\tau}\rangle
\end{aligned} \tag{10}$$

where ε is the τ detection efficiency and BR the total branching ratio of the τ decay channels to which the experiment is sensitive. The sensitivity to oscillations can be determined by evaluating the mean values in equation (10) as a function of Δm^2 and $\sin^2 2\theta$. $\langle \varepsilon_\tau \rangle$ and $\langle \sigma_\tau \rangle$ include the convolution of the ν_μ spectrum with the oscillation probability. $\langle P_{\mu\tau} \rangle$ only depends on the ν_μ spectrum and can be written, in the usual two-flavour approximation, as

$$\langle P_{\mu\tau} \rangle = \sin^2 2\theta \langle \sin^2 \frac{1.267 \Delta m^2 L}{E} \rangle$$

If the experiment does not observe any event, with no expected background, the 90% C.L. upper limit for the signal amounts to 2.44 observed events[13)]. For large Δm^2 values equation (10) assumes the asymptotic form

$$\sin^2 2\theta \leq \frac{2 \times 2.44 \langle \varepsilon_\mu \rangle \langle \sigma_\mu \rangle}{N_\mu \langle \varepsilon_\tau \rangle \langle \sigma_\tau \rangle BR} \tag{11}$$

From equation (11) we deduce that in the absence of background the sensitivity of a *direct appearance* experiment linearly improves with the number of detected ν_μ charged current events. The asymptotic limit for Δm^2 has an expression analogous to equation (9).

2.3. Short baseline versus long baseline appearance experiments

Experiments searching for neutrino oscillations with accelerator beams are usually classified as “short” or “long” baseline according to the distance L of the detector from the neutrino source.

The solid angle subtended by a detector with transverse area A respect to the neutrino direction and located at distance L from the source is $\Delta\Omega = A/L^2$, under the hypothesis of detector transverse dimensions smaller than L. Neutrinos are produced by mesons with a given energy E_m and are emitted at an angle $\cos\theta = (\cos\theta^* + \beta)/(1 + \beta\cos\theta^*)$ with respect to the meson flight direction, being θ^* the decay angle in the centre of mass and β the velocity of the parent meson in the laboratory system. Obviously, the larger is the solid angle subtended by the detector the higher is the probability for a neutrino to cross the detector. Therefore, similarly to the solid angle, also the neutrino flux $\phi_\mu(E)$ goes like $1/L^2$.

Let's now consider an experiment searching for $\nu_\mu \leftrightarrow \nu_\tau$ oscillations which is background free. In the case of a negative search (equation (11)) the minimum $\sin^2 2\theta$ to which the experiment is sensitive is proportional to the inverse of the number of detected events (N_μ), in turn proportional to L^{-2} and to the detector mass M_d

$$N_\mu = N_a M_d \int \phi_\mu(E) \sigma_\mu(E) \varepsilon_\mu(E) dE \simeq \frac{N_a M_d}{L^2} \int f(E) \sigma_\mu(E) \varepsilon_\mu(E) dE \tag{12}$$

	No background	Background
$\sin^2 2\theta$	$\propto L^2; \propto 1/M_d$	$\propto L; \propto 1/\sqrt{M_d}$
Δm^2	No L dependence; $\propto 1/\sqrt{M_d}$	$\propto 1/\sqrt{L}; \propto 1/\sqrt[4]{M_d}$

Table 1. Dependence of the oscillation parameter on the experimental parameters.

where $f(E)$ is a function which takes into account the energy dependence of the neutrino flux and N_a is the Avogadro number. The sensitivity to $\sin^2 2\theta$ goes quadratically with the distance source-detector and it is proportional to the inverse of the detector mass. Concerning the sensitivity to Δm^2, by using equations (9), (11) and (12) we obtain

$$\Delta m^2 \lesssim \sqrt{\frac{2.44\langle\varepsilon_\mu\rangle\langle\sigma_\mu\rangle}{\int N_a M_d f(E)\sigma_\mu(E)\varepsilon_\mu(E)dE} \times \frac{1}{\langle\varepsilon_\tau\rangle\langle\sigma_\tau\rangle BR} \times \frac{E^2}{1.267}}$$

Therefore, the sensitivity to Δm^2 for a background-free appearance experiment only depends on the neutrino beam energy and on the number of collected interactions and not on the baseline L. It is important to stress that the sensitivity to Δm^2 improves with the square-root of the detector mass: $\Delta m^2 \propto 1/\sqrt{M_d}$.

In the presence of background the scenario is slightly modified. As an example, let's consider a $\nu_\mu \leftrightarrow \nu_e$ indirect appearance search. In that case, an irreducible background may be given by the intrinsic contamination of electron neutrinos in the beam. The sensitivity to $\sin^2 2\theta$ is proportional to the square-root of the expected background and proportional to the inverse of the observed number of events (assuming $N_\mu \gg \sqrt{N_e}$). Therefore, being both N_μ and N_e proportional to L^{-2} and M_d, $\sin^2 2\theta$ becomes proportional to $L/\sqrt{M_d}$. This means that the sensitivity to $\sin^2 2\theta$ improves linearly with decreasing the distance source-detector. On the other hand, it can be easily shown that the sensitivity to Δm^2 improves with the square-root of L and with the fourth-root of M_d.

An interesting case is when the expected background is very small ($\mathcal{O}(1)$ event). In this condition Poisson statistics has to be considered to set the upper limit on the observed number of events. It can be shown that, by following the Feldman and Cousins approach [13)], if an experiment has an expected background of 0.1 events, an increase in statistics by a factor 10 improves the sensitivity to $\sin^2 2\theta$ by only 30%. In Table 1 the sensitivities to Δm^2 and $\sin^2 2\theta$ are shown as a function of L and M_d.

From the above discussion it follows that the relevant parameter to be varied in order to explore a given $\Delta m^2 - \sin^2 2\theta$ region is the baseline L, being weaker the dependence of the experimental sensitivity on the detector mass. In the ideal case of a background free experiment, the detector should be located as near as possible to the neutrino source, with the highest possible mass, in order to increase the number of observed events and therefore the sensitivity to $\sin^2 2\theta$. The sensitivity to Δm^2 is independent of L, but one could benefit from a large detector mass.

In real life, unfortunately, the presence of background is unavoidable. Therefore, depending on the $\Delta m^2 - \sin^2 2\theta$ region to be tested, two complementary approaches can be envisaged for typical experimental conditions:

- a detector, $\mathcal{O}(1\ ton)$ mass, with high background rejection power located at short distance from the source ("short baseline"). The collected statistics can be large, with small background, so allowing to explore small mixing angles ($\sim\ 10^{-4} - 10^{-5}$) despite the limited sensitivity to Δm^2 ($\sim\ 1\ eV^2$). In order to keep the background low, short baseline experiments require high granularity detectors, to exploit the topology of the interaction, and good kinematical reconstruction capabilities;

- a large mass detector ($\mathcal{O}(1000\ ton)$) with moderate background rejection power located at large distance from the source ("long baseline"). Since $N_\mu \propto M_d/L^2$, the ratio of background events between typical long and short baseline experiments is

$$\frac{N_{long}}{N_{short}} \simeq \frac{(1000\ ton) \times (1\ km)^2}{(1\ ton) \times (1000\ km)^2} = 10^{-3}$$

  A background rejection factor three orders of magnitude lower than for a short baseline experiment is still enough to keep the background low and to explore small Δm^2 regions ($\sim\ 10^{-3} - 10^{-4}\ eV^2$). The allowance for moderate background rejection allows to deal with massive detectors with poor granularity, to partially compensate for the large flux reduction.

In summary, short baseline experiments (small mass, high granularity, efficient kinematical reconstruction) are more suitable to explore small mixing angles. Conversely, long baseline detectors (large mass, coarser granularity, limited kinematical reconstruction capability) can allow to probe small Δm^2 domains. However, as we will see later, "high granularity" detectors are better suited for $\nu_\mu \leftrightarrow \nu_\tau$ direct-appearance searches. This feature implies high efficiency in the detection of the τ lepton, signature of the oscillation process. The high efficiency, consequently, allows the use of relatively low mass targets.

3. The CERN-Gran Sasso neutrino beam (NGS)

We mentioned that the experimental results on the atmospheric neutrino anomaly motivated the design of a series of facilities able to provide neutrino beams for LBL experiments. As an example, we mention the proposed NGS beam [12)] from the CERN SPS directed towards the INFN Gran Sasso Laboratory, situated underground in central Italy, 732 km from CERN. The project is presently in the process of the

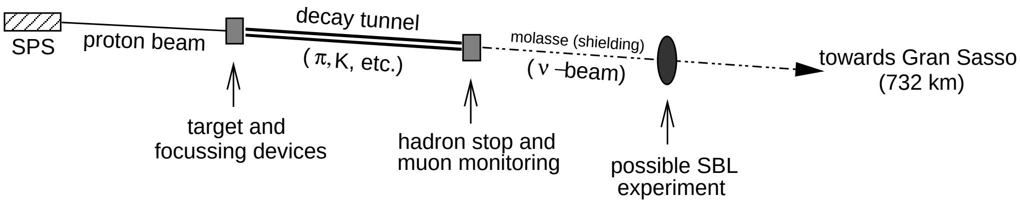

Fig. 1. Schematic layout of the NGS neutrino beam line.

scientific and financial evaluation by the CERN and INFN Committees. In case of approval its commissioning is expected by early 2005.

Similarly to its predecessor, the WANF [14], the NGS neutrino beam is produced by the decay of mesons, mostly π and K, originating from the high-energy, high-intensity SPS proton beam hitting a suitable target. The main components of the beam-line are schematically shown in Fig. 1.

The SPS accelerator is being modified for its future role of LHC injector, while continuing to provide protons and ions for fixed target experiments. The extraction system foreseen for the LHC allows fast-extracted pulses (up to 20 μs) to be sent to the TI8 transfer line towards the LHC. With some modifications to permit two fast extractions per cycle, this system can also be used to extract protons onto the NGS target.

The total length of the proton beam from the SPS to the NGS target is 830 m, and its momentum 400 GeV. The beam branches off the TI8 beam after 110 m. The necessary deflection (horizontal and vertical) to reach the direction towards the Gran Sasso Laboratory is achieved by 73 bending magnets.

The proton target is based on the successful design of the target used for the WANF. In an aluminium container 11 rods of graphite, 10 cm long and 3 mm diameter each, constitute a 2 m long target array. The change from beryllium (WANF) to graphite has been mainly motivated by the change from fast-slow (6 ms) to fast (10 μs) proton beam extraction and by the better thermo-mechanical properties of graphite.

The WANF experience is the origin of the choice for the focusing elements, horn and reflector, two coaxial lenses similar in shape but different in size. The distances of horn and reflector from the target and the shape of the magnetic field provided by them were originally chosen to optimise a wide-band high-energy ν_μ beam, a configuration which yields high intensity.

Typical π decay lengths, 2.2 km at 40 GeV, make a long decay tunnel desirable. Given the angular distribution of the mesons which can produce neutrinos, the longer the decay tunnel is, the larger has to be its diameter. For the NGS, a tunnel of 2.45 m diameter and 1000 m length has been chosen, followed by a hadron stopper.

The detection of the signals induced by muons produced in the meson decays in a set of silicon detectors allows an "on-line" monitoring and tuning of the beam. The monitoring system consists of two arrays of silicon detectors measuring the muon flux penetrating the hadron stopper and the hadron stopper plus a 67 m thick region of molasse. The separation of the two planes, equivalent to 25 m of iron, allows a rough measurement of the muon energy spectrum. Moreover, some knowledge about the beam angular distribution can also be obtained.

The original NGS "reference" neutrino beam from the CERN SPS to the Gran Sasso is described in [12]. A further optimisation of the ν_τ interaction yield was originally proposed in [15], contributing to the new NGS beam design developed by the CERN/INFN Technical Committee [16].

4. Optimisation for $\nu_\mu \leftrightarrow \nu_\tau$ oscillation search

The NGS reference beam was not far from optimum for a $\nu_\mu \leftrightarrow \nu_\tau$ appearance search. However, it was expected that an optimisation of the target/horn/reflector system could yield a gain in flux of oscillated neutrinos [15]. We have seen that, since the appearance of the ν_τ is detected through its CC interaction with the experimental target, this neutrino must be energetic enough ($\sim 3.5\ GeV$) to produce its τ lepton partner. This sets a lower limit to the energy of the neutrino beam. The ratio of cross sections (σ_τ/σ_μ) increases slowly; therefore, a high-energy beam is more suitable for a $\nu_\mu \leftrightarrow \nu_\tau$ appearance search. On the other hand, the fact that the preferred Super-Kamiokande value for Δm^2 lies in the region of a few $10^{-3}\ eV^2$ leads to a somehow "low" energy of the ν_μ oscillating into ν_τ, as shown in the following.

The number of τ leptons observed in a given detector is given by

$$N_\tau = N_a M_d \int \phi_\mu(E) P(\nu_\mu \leftrightarrow \nu_\tau)(E) \sigma_\tau(E) \epsilon(E)\ \mathrm{d}E$$

where ϕ_μ is the ν_μ flux at the detector site, $P(\nu_\mu \leftrightarrow \nu_\tau)(E)$ is the oscillation probability between ν_μ and ν_τ, σ_τ is the ν_τ CC interaction cross section, ϵ is the τ detection efficiency, N_a is the Avogadro number and M_d is the detector mass. In Fig. 2 we plot σ_τ and σ_μ as a function of E and their ratio, while in Fig. 3 P is plotted against E in the case of $L = 732\ km$, full mixing and for different Δm^2 values. One can already see that σ_τ increases with increasing beam energy, unlike the oscillation probability.

The ν_τ cross section can be parametrised as

$$\sigma_\tau = \sigma_0 E f_\tau(E)$$

where $\sigma_0 = 0.67 \times 10^{-38}\ cm^2/GeV$. Therefore, the number of ν_τ interactions may be expressed as

$$N_\tau = N_a M_d sin^2 2\theta \sigma_0 \int \phi_\mu(E) \sin^2(\frac{1.27 L \Delta m^2}{E}) f_\tau(E) \epsilon(E) E dE$$

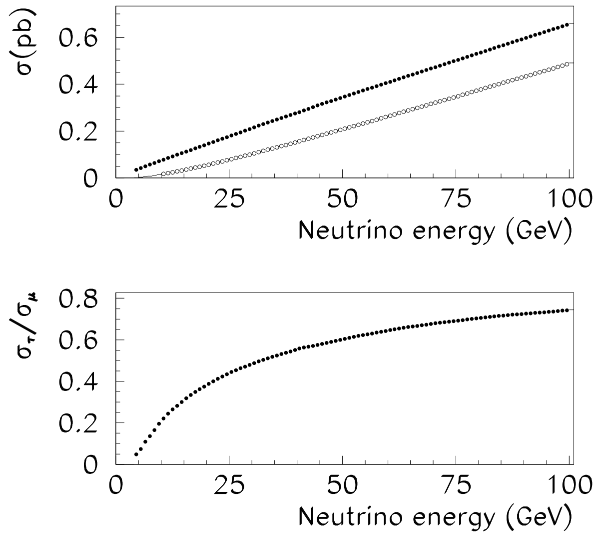

Fig. 2. Top: $\sigma_{\nu_\tau}(E)$ (open circles) and $\sigma_{\nu_\mu}(E)$ (black circles) as a function of the neutrino energy; bottom: the $\sigma_{\nu_\tau}(E)/\sigma_{\nu_\mu}(E)$ ratio. DIS, QE and resonances have been included.

If the condition $\Delta m^2 L/E \ll 1$ holds (in the hypothesis of small Δm^2)

$$N_\tau \sim N_a M_d \sin^2 2\theta (1.27 \Delta m^2 L)^2 \sigma_0 \int \phi_\mu(E) f_\tau(E) \epsilon(E) dE/E$$

As a consequence of that, the τ yield optimisation becomes independent of the actual Δm^2 value. One could think that the quantity to be maximised, in order to take advantage of the long baseline configuration, is the average of $f_\tau(E)\epsilon(E)/E$ over the beam energy spectrum. Fig. 4 shows the ratio $f_\tau(E)/E$ as a function of E. A neutrino beam spectrum peaked around 10 GeV would seem to be the correct choice. However, this does not take into account the effect of the neutrino flux $\phi_\mu(E)$ and of the τ detection efficiency $\epsilon(E)$ of the experiments.

In Fig. 5 the energy spectrum of the NGS beam is shown under the assumption of ideal focusing of all the mesons produced at the target. If one convolutes the function $f_\tau(E)/E$ with the one in Fig. 5, the yield of ν_τ CC interactions rises steeply up to ~ 10 GeV and stays rather constant up to $20-25$ GeV, as shown in Fig. 6. The area covered in Fig. 6 by a real focusing system should be as large as possible.

With the above guideline principles, the NGS beam has been optimised for ν_τ appearance experiments at Gran Sasso [16]. The main changes are:

- an increased average proton current during fixed-target operation by a more efficient use of the SPS;

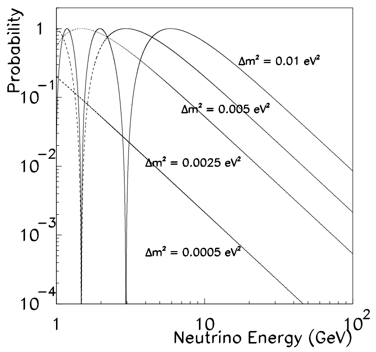

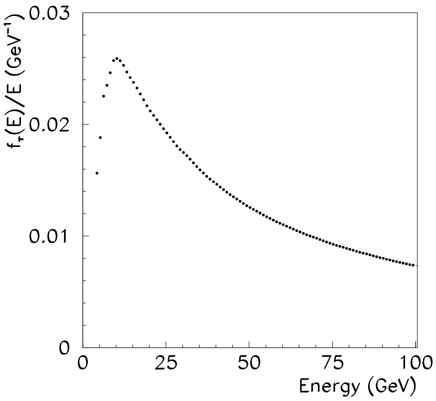

Fig. 3. (left) Oscillation probability (full mixing and L=732 km) as a function of the energy for different Δm^2 values.

Fig. 4. (right) $f_\tau(E)/E$ as a function of E. DIS, QE and resonances are included.

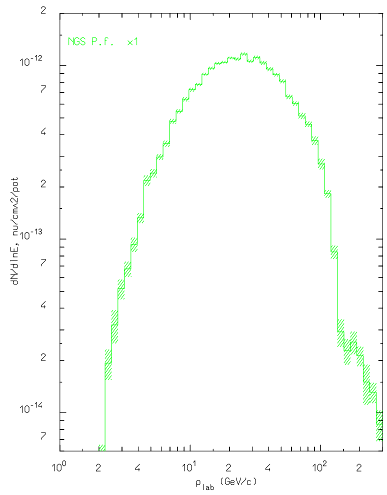

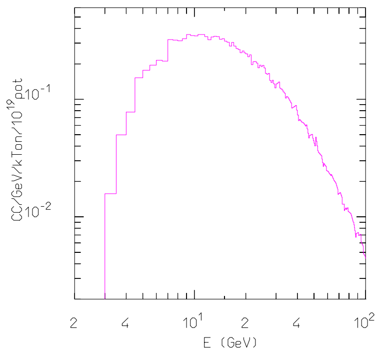

Fig. 5. (left) Neutrino fluxes at the Gran Sasso for the NGS beam in the hypothesis of "ideal" focusing.

Fig. 6. (right) The function dN$_\tau$/dE is plotted for Δm^2=2.5 $\times$ 10^{-3} eV^2 in the hypothesis of "ideal" focusing. This function is proportional to $\phi_\mu(E)$ $f_\tau(E)/E$, in the limit of small Δm^2. In this limit its shape is independent of Δm^2 while the total number of events scales with $(\Delta m^2)^2$. Note the logarithmic energy scale.

- LHC operates in parallel with the NGS and its effect has to be taken into account;
- an increased rate of ν_τ CC events per proton on target obtained by
  - changing the secondary beam optics to improve the acceptance and to optimise the shape of the spectrum;
  - increasing the current in the co-axial lenses (horn and reflector);
  - reducing the amount of material in the secondary beam (pions, kaons).

The result is an increase of about a factor three in the number of expected charged current ν_τ events per year at Gran Sasso, when compared to the initial design [12].

Concerning the proton yield, the boundary conditions for SPS running were carefully studied. After publication of the NGS report [12], it was found that the preparation procedures for RF equipment could be shortened by $0.2\,s$. This permits the shortening of the NGS cycles with two fast extractions at $400\,GeV/c$ from 6.2 to $6.0\,s$. The gain for the NGS is more striking: a cycle of $1.2\,s$ is dictated by the PS injector complex, hence the SPS cycle time for NGS is reduced from $7.2\,s$ [12] to $6.0\,s$. This has a considerable impact on the protons on target $(pot)/year$ for the NGS.

Since the energy of the proton beam for the slow extraction users will be $400\,GeV/c$ in the future (budgetary reasons), the power dissipation in the SPS magnets is no longer relevant and longer super-cycles leading to larger numbers of $pot/year$ for the NGS can be envisaged. On the other hand, the operation of the LHC will have an impact on the SPS availability for the NGS. Taking all these factors into account, the expected proton intensity on the NGS target is $4.5 \times 10^{19}\,pot/year$, when operating in parallel with the LHC. This number should be compared with the upper limit, namely the performance in dedicated operation which would provide $7.6 \times 10^{19}\,pot/year$ assuming 200 days of operation per year. This indicates a significant loss (40 %) due to sharing.

The resulting NGS beam performance for the new reference beam is summarised in Table 2. The expected number of interacting ν_τ for $\sin^2 2\theta = 1$ and three values of Δm^2 is shown in Table 3. When compared to [12], a substantial increase of about a factor of two in the expected ν_τ events per proton is found, leading to an improved performance by a factor of three in ν_τ per $kton$ and per $year$.

5. The Fermilab NuMI neutrino beam

Another neutrino beam facility for long baseline experiments, exploiting the Main Injector, is foreseen from Fermilab to the Soudan Mine in Minnesota [6]. As in the case of the NGS, the distance source-detector is about $730\,km$. This project has been approved and the beam is expected to be commissioned by the year 2002. The map of the neutrino beam is shown in Fig. 7.

Energy region E_{ν_μ} [GeV]	1 - 30	1 - 100
ν_μ [m^{-2}/pot]	7.1×10^{-9}	7.45×10^{-9}
ν_μ CC events/pot/kton	4.70×10^{-17}	5.44×10^{-17}
$\langle E \rangle_{\nu_\mu\, fluence}$ [GeV]		17
fraction of other neutrino events:		
ν_e/ν_μ	0.8 %	
$\overline{\nu}_\mu/\nu_\mu$	2.0 %	
$\overline{\nu}_e/\nu_\mu$	0.05 %	

Table 2. Expected performance of the new NGS reference beam.

Energy region E_{ν_τ} [GeV]	1 - 30	1 - 100
$\Delta m^2 = 1 \times 10^{-3}\,\mathrm{eV}^2$	2.34	2.48
$\Delta m^2 = 3.5 \times 10^{-3}\,\mathrm{eV}^2$	~ 29	~ 30
$\Delta m^2 = 5 \times 10^{-3}\,\mathrm{eV}^2$	~ 58	~ 60

Table 3. Expected number of ν_τ CC events at Gran Sasso per kton and per year. Results of simulations for different values of Δm^2 and for $sin^2(2\theta) = 1$ are given. These numbers do not take detection efficiency into account.

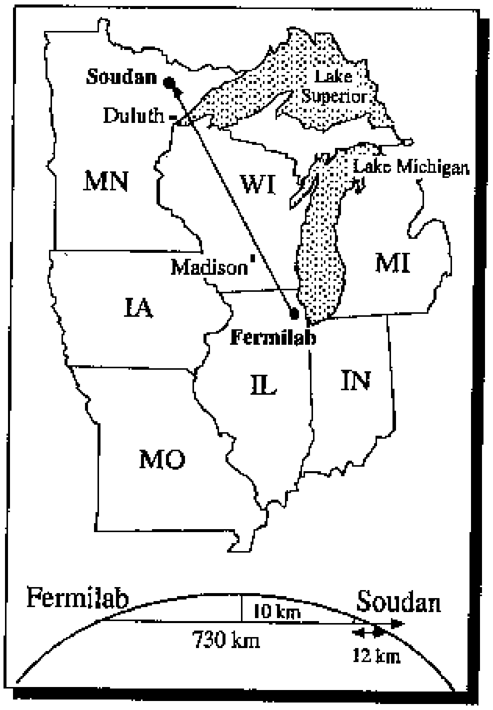

Fig. 7. The trajectory of the MINOS neutrino beam between Fermilab and Soudan.

The main feature of the NuMI beam is the possibility to have a neutrino energy spectrum which could extend from 1 to 20 GeV, allowing to explore different Δm^2 domains. Since magnetic focusing systems have limited momentum acceptance, different spectra can be obtained by changing the position of the horn and reflector along the beam-line and adopting different targets. Three different beams have been designed and their features are shown in Fig. 8 together with the spectrum corresponding to perfect focusing.

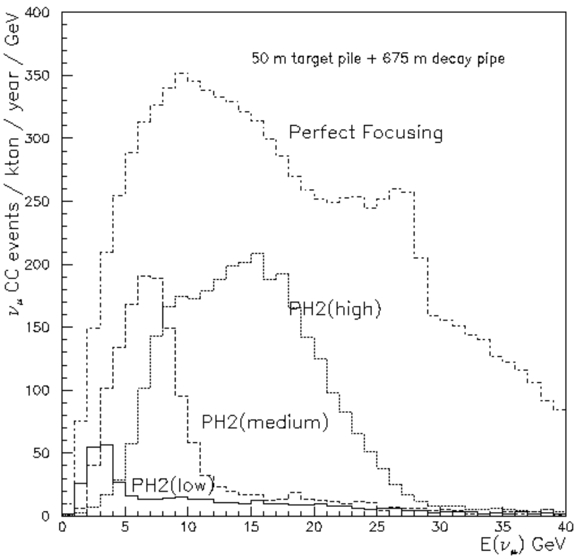

Fig. 8. Comparison of the event rates at Soudan in the case of perfect focusing, and rates achieved with three beam design configurations.

The neutrino beam is obtained by shooting 120 GeV protons accelerated by the Fermilab Main Injector with a repetition rate of 1.9 s onto a beryllium (or graphite) target about 160 cm long. The Main Injector is expected to deliver about 4×10^{13} pot over 1 ms. The hadrons produced in the target are focused by two parabolic magnetic lenses and transported through an evacuated beam pipe, 1 m in radius and 675 m long. The shielding for the near detector against muons is provided by a hadron absorber placed downstream from the beam pipe and by dolomite rock between the absorber and the near detector location. The main characteristics and the expected

Proton Energy	Proton/pulse	Cycle time	pot/year	$\langle E_\nu \rangle$
120 GeV	4×10^{13}	1.9 s	3.6×10^{20}	$3 - 16\ GeV$

Table 4. NuMI beam features and expected performance. The average energy goes from 3 GeV for the PH2 (low) beam to 16 GeV for the PH2 (high) beam.

$events/(10^{19} pot \times kton)$	Low energy	Medium energy	High energy
ν_μCC	12.4	38.9	86.7
ν_eCC	1.5×10^{-1}	3.5×10^{-1}	4.9×10^{-1}
$\bar{\nu}_\mu$CC	1.7	1.2	9.2×10^{-1}
$\bar{\nu}_e$CC	3.5×10^{-2}	2.4×10^{-2}	2.4×10^{-2}
ν_τCC at $\Delta m^2 = 0.01\ eV^2, \sin^2 2\theta_{\mu\tau} = 1$	7.3×10^{-1}	3.6	8.4
ν_τCC at $\Delta m^2 = 0.001\ eV^2, \sin^2 2\theta_{\mu\tau} = 1$	1.4×10^{-2}	7.0×10^{-2}	1.1×10^{-1}

Table 5. Summary of neutrino rates at the Soudan location for the three possible beams.

performance of the NuMI facility are shown in Table 4. Event rates are given in Table 5.

6. Future long baseline experiments

In the next sessions we will review some of the proposed experiments for the NGS and NuMI facilities, aiming at a search for $\nu_\mu \leftrightarrow \nu_\tau$ oscillation in appearance mode, as described in Sections and . We sort the experiments with decreasing the "detection efficiency", starting with nuclear emulsion and ending with water Cerenkov. This efficiency is ultimately related to the granularity of the detection technique.

It is important to stress that the performance presented in the following for the NGS experiments refer to the LoI's submitted to the SPSC and LNGSC in 1998. The improvement in the NGS design performance discussed above has not been taken into account.

7. The OPERA experiment in the NGS beam

In the last years, we have observed the ribirth of the nuclear emulsion technique. The use of a large mass emulsion target for the CHORUS experiment [17] has been made possible by the progress of the scanning devices, nowadays exploiting completely automatic microscopes [18]. This has permitted a next generation of emulsion detectors to be conceived for $\nu_\mu \leftrightarrow \nu_\tau$ oscillation searches with appearance experiments [19][20][10].

The starting point in the design of OPERA is the Emulsion Cloud Chamber (ECC) [21,22,23,24]. The ECC provides a massive target made up of a sandwich of dense passive material plates and thin emulsion sheets (ES). Employing metal plates as a target with the emulsion used only for tracking, the detector mass can be increased by orders of magnitude as compared to conventional emulsion experiments. The

OPERA concept [10] is an evolution of the ECC. The idea is to insert a "gap" between consecutive emulsion sheets (Fig. 9). This "empty" space between the ES allows direct detection of the short-lived τ decay kink, which makes this approach superior to the impact parameter measurement done with the standard ECC, and therefore yielding a substantial background reduction.

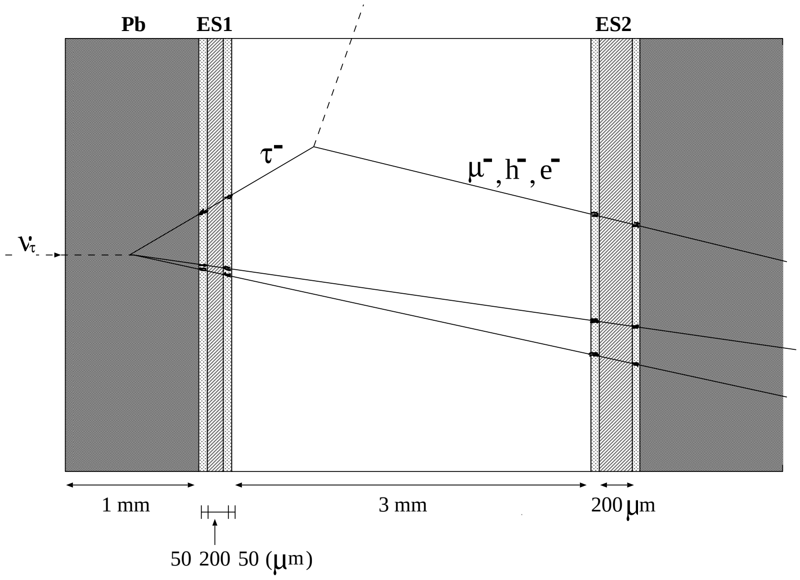

Fig. 9. Schematic structure of the OPERA target. The τ decay kink is directly reconstructed in space by using four track segments in the emulsion sheets ES1 and ES2.

The present design of the future OPERA detector is a lead/emulsion target subdivided into "bricks". Each brick, weighting about 8 kg, has dimensions orthogonal to the beam direction of 15 $\times$15 cm^2. It consists of a sequence of 30 sandwiches, each composed of a 1 mm thick lead plate followed by an emulsion sheet (ES1), a spacer of 3 mm, and another emulsion sheet (ES2) as shown in Fig. 9. ES are made up of a pair of emulsion layers 50 μm thick, on a 200 μm plastic base. The spacer consists of very low density material. Charged particles give two track segments in each ES. The $\sim$ 1 μm granularity of the emulsion layers ensures redundancy in the measurement of particle trajectories. A matrix of adjacent bricks, arranged in a plane structure, forms a target module. The modularity of the target allows to conceive a total target mass (lead) of $\sim$ 1000 ton, suited to meet the physics goal of the experiment. The target structure also permits the removal of those bricks where an interaction took place and to analyse their emulsion sheets soon after.

If a τ is produced, it will decay within a few millimetres, either in the lead plate or, *e.g.* in the low density spacer between ES. For decays in the spacer the τ is detected by measuring the angle between the charged decay daughter and the τ directions (kink). For its measurement, the directions of the tracks before and after the kink are reconstructed (in space) by means of the first pair of ES downstream of the lead plate where the primary vertex occurred (Fig. 9).

Electronic detectors, placed behind each target module, are needed to identify the actual brick where the neutrino interaction took place and to guide the scanning. OPERA at the Gran Sasso is naturally shielded against non-penetrating particles and it is exposed to a neutrino beam without halo muons. This leads to a low density of background tracks "stored" in the emulsion and removes the need for a precise location of individual tracks in the ES by electronic trackers. Therefore, a moderate space resolution can be tolerated.

The performance requirements for the electronic detectors are: $\sim 0.5 - 1\ cm$ space accuracy, high efficiency and long term reliability. The preferred option for the OPERA target is based on narrow scintillator strips read-out by WLS fibres coupled to photo-detectors. Magnetised iron toroids placed downstream of the target, have the task of identifying muons with high efficiency and measuring their charge for background reduction. The trackers for the muon system must have the space resolution of $\sim 1\ mm$.

One option for the muon system consists of 5 cm thick toroidally-magnetised octagonal steel plates arranged in $\sim 75\ cm$ long magnet modules. The magnetisation coils run through a 10 cm hole at the centre of each plate in a module. The average B-field in iron is about 1.5 T. Each plate is followed by a 1 cm thick plane of plastic scintillator strips with WLS fibre read-out. The calorimetrised magnets act as a hadronic tail catcher and, in addition, have muon tracking and ranging capabilities. Several target modules followed by a muon spectrometer constitute a supermodule, which is schematically depicted in Fig. 10. The total detector mass will be obtained by a suitable number of supermodules.

7.1. Event and detection efficiency

The signal of the occurrence of $\nu_\mu \leftrightarrow \nu_\tau$ oscillations is the ν_τ CC interactions in the detector target: $\nu_\tau N \rightarrow \tau^- X$. The detection of the τ lepton decay in the final state identifies this reaction through the decay modes into single hadron, muon and electron: $\tau^- \rightarrow h^- \nu_\tau (n\pi^0)$, $\tau^- \rightarrow \mu^- \nu_\tau \overline{\nu}_\mu$, $\tau^- \rightarrow e^- \nu_\tau \overline{\nu}_e$.

Several elements contribute to determine the τ detection efficiency. The first is the probability of the τ decaying in the spacer. The second is given by the rejection of small-angle ($< 20\ mrad$) and very large-angle kinks ($> 500\ mrad$). The lower cut is due to the angular resolution (5 $mrad$) in the measurement of the kink angle in space by means of the four track segments in the ES. The upper cut is motivated by considerations related to the scanning efficiency. The fraction ϵ_{kink} of τ decays with a kink angle in the useful range depends on the actual decay mode. Another factor is the geometrical detection efficiency ϵ_{geom} due to the fiducial volume cut of $\sim 90\%$, which has to be applied to take into account edge effects in the ES scanning.

The global detection efficiency of OPERA, multiplied by the branching ratios of the single-prong τ decay channels, is high if compared to other experiments and allows

Background source	evts/10^3 CC	after kinematics
π and K decays	0.03	–
re-interactions	< 0.01	–
charm	0.13	0.06
TOTAL	0.16	0.06

Table 6. Number of background events (per 1000 CC events), for the different channels.

for a comparatively low target mass. It amounts to $\sim 30\%$ for $\Delta m^2 = 3.5 \times 10^{-3}\ eV^2$ and full mixing, the oscillation parameters corresponding to the best fit of the Super-Kamiokande data.

7.2. Background

The expected background sources are the decay of pions and kaons produced in CC and NC ν_μ interactions and the 1-prong decay of charmed particles. The decay in the spacer of pions and kaons produced in NC neutrino interactions can fake the topology of a candidate τ event. CC interactions are an additional source for this background if the prompt primary muon is undetected. The expected number of these background events is $3{\times}10^{-5} \times N_{CC}$, where N_{CC} is the total number of CC neutrino interactions collected by OPERA.

Charmed particles are produced in neutrino interactions through the reactions: a) $\nu_\mu N \to c\,\mu X$, b) $\nu_\mu N \to c\bar{c}\,\mu X$, c) $\nu_\mu N \to c\bar{c}\,\nu_\mu X$. These processes may constitute a background to the oscillation signal if one fails to detect the primary muon (a-b) or the charm partner (b-c). The most relevant source is given by single charm production (reaction (a)), since charmed mesons have mass and lifetime similar to those of the τ. If the primary muon is missed, a D^+ meson decaying in one charged particle (plus neutrals) can fake a genuine τ event, since the (positive) sign of the D^+ daughter is only measured for the muonic channel by the muon spectrometers.

For the three 1-prong τ decay modes together OPERA will be left with $\sim 16{\times}10^{-5} N_{CC}$ background events (Table 6). Candidate events will undergo further kinematical analysis at the interaction and decay vertices. The expected difference in the kinematics of τ decays with respect to background events is then exploited. An additional background rejection of a factor $\sim$ 2 is estimated (Table 6), keeping high efficiency for the signal. The total estimated background amounts to $\sim$ 0.4 events with an overall uncertainty of about 20%, under the assumption of 16×10^{19} *pot* from the NGS.

7.3. Sensitivity

The number of detected ν_μ CC interactions in OPERA is $\sim$ 7000. The 90% C.L. upper limit on the mixing angle (for large Δm^2) is $\sin^2 2\theta_{\mu\tau} <\sim 4 \times 10^{-3}$ under the hypothesis of no observed events and $\sim$ 0.4 estimated background events [13]. The corresponding minimum Δm^2 (for full mixing) is $\sim\ 1 \times 10^{-3}\ eV^2$. The exclusion plot is shown in Fig. 11 together with the parameter region allowed by the combined analysis of the Super-Kamiokande data [28].

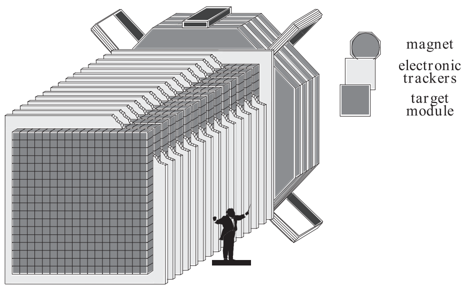

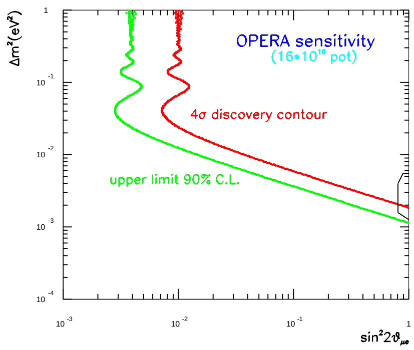

Fig. 10. (left) The concept of the OPERA detector supermodule.

Fig. 11. (right) Sensitivity of OPERA in the search for $\nu_\mu \leftrightarrow \nu_\tau$ oscillations. The 90% C.L. limits is plotted together with the 4σ discovery contour. The region allowed by the recent Super-Kamiokande[28] data is also shown.

OPERA is an experiment designed for discovery. Assuming 16×10^{19} *pot* and $\nu_\mu \leftrightarrow \nu_\tau$ oscillations with the best fit Super-Kamiokande parameters, about $\sim\ 20\ \tau$ would be detected with an expected background of $\sim\ 0.4$ events. Since the unambiguous experimental signature leads to a very low background, these numbers quantify the discovery. In Fig. 11 the 4σ discovery contour is plotted. For full mixing, it corresponds to $\Delta m^2 = 1.8 \times 10^{-3}\ eV^2$.

8. The ICARUS detector

The ICARUS Collaboration [7] has been developping, over the last two decades, a liquid argon time projection chamber (TPC) detector with bubble-chamber-like space resolution. The physics goals which can be addressed by this technique include proton decay searches, solar and atmospheric neutrino detection and neutrino oscillations with a long baseline beam, *e.g.* with the future NGS beam.

The principle of the ICARUS detector is the following: a large liquid argon volume is contained in cryostats; each cryostat (Fig. 12) has two wire readout planes, one at each end of the volume, a high-voltage plane at the centre and a maximum drift length of 1.5 m. Electrons produced by charged particles crossing the detector are collected on the readout planes, each of those has three coordinates at 60° from each other and readout wire pitch of 3 mm. This corresponds to a *bubble* diameter of about of 3 mm, which was, for instance, the figure of Gargamelle.

The detector is a homogeneous tracking device, capable of dE/dx measurement. The high dE/dx resolution allows good momentum measurement and particle identification for soft tracks. Electromagnetic and hadronic showers are fully sampled. This gives good energy resolution for electromagnetic $(\sigma(E)/E \approx 3\%/\sqrt{E(GeV)})$ and hadronic *contained showers* $(\sigma(E)/E \approx 12\%/\sqrt{E(GeV)})$. ICARUS also features excellent electron identification and $e - \pi^0$ separation.

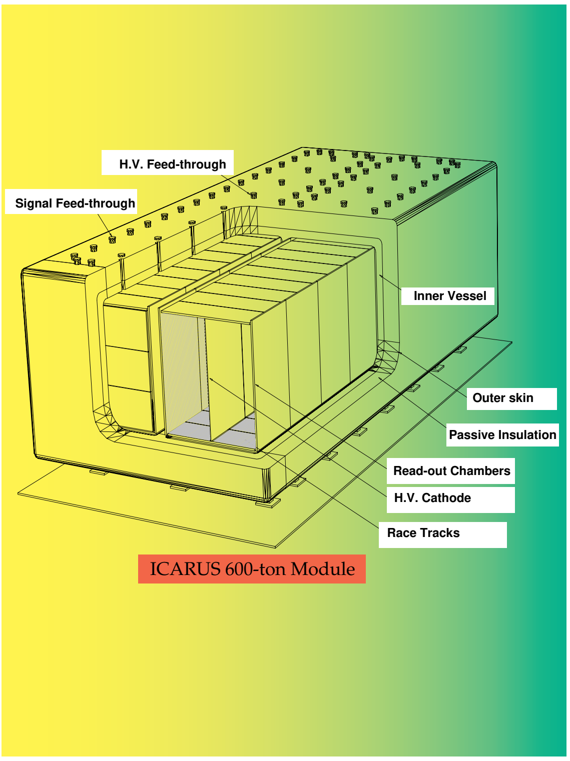

Fig. 12. Schematic view of the 600 *ton* ICARUS detector.

Fig. 13. A neutrino interaction in the 50 *litres* prototype of the ICARUS detector.

A small prototype (50 *litres*) of the ICARUS detector has been successfully exposed to the WANF neutrino beam. The display of a detected neutrino event is shown in Fig. 13. A larger module of 600 *ton* is under construction and expected to be operational by the year 2000 at the Gran Sasso Laboratory.

For the future, two scenarios have been envisaged. The first one foresees the realization of a 2.4 *kton* detector made of four 600 *ton* modules [7]; we refer to it as

ICARUS. The second scheme foresees a single module of 30 *kton* liquid argon to be installed either in one of the Gran Sasso caverns or outside, in the NGS beam-line (SUPER-I [25)]).

8.1. The ICARUS experiment in the NGS beam

The ICARUS $\nu_\mu \leftrightarrow \nu_\tau$ oscillation sensitivity has been detrmined considering four modules (2.4 *kton*). Because of the high resolution in measuring kinematical quantities, the $\nu_\mu \leftrightarrow \nu_\tau$ appearance search is based on the kinematical suppression of the background by using methods analogous to those of the NOMAD experiment [26)]. The basic idea consists in reconstructing the transverse missing momentum due to the undetected neutrino(s) produced in τ decays. Since this missing transverse momentum is approximately Lorentz invariant, the τ detection efficiency should be constant as a function of the ν_τ energy. Nevertheless, a slight decrease with increasing energy is expected, since the cuts applied to isolate the ν_τ events depend on the background rate, which in turn is a function of the neutrino energy.

Estimates are available for the $\tau \to e$ channel whose detection efficiency times branching ratio has been evaluated to be about 0.09. The main background sources for the electron channel are the ν_e contamination of the ν_μ beam and the π^0 misidentified as electrons in neutral current events. The rejection power of the latter is close to 100%. A ν_e event is a background either if there are undetected neutral hadrons in the final state or because of the smearing due to nuclear effects in the target nucleon and to the detector resolution. It has been shown that a background rejection factor of about of 100 is sufficient to obtain just one background event [7)].

The SUPER-I detector is an evolution of the 600 *ton* ICARUS module. It is a single liquid argon 30 *kton* module, linearly extrapolated from the 600 *ton* module by a factor $\sqrt[3]{30\ kton/0.6\ kton} = 3.68$. The aim of such a detector is twofold. The first one is to perform a LBL experiment able to detect events even at small Δm^2 ($\sim 1\times10^{-3}$) in order to safely cover the allowed Super-Kamiokande parameter region. The second one is to explore the same region by using atmospheric neutrinos.

A detailed study of all inefficiency and background sources has been carried out for the following decay channels: $\tau^- \to e^-$, $\tau^- \to h^-(n\pi^0)$, $\tau^- \to \rho^-$ and $\tau^- \to h^-h^-h^+(n\pi^0)$. It is worth mentioning that hadrons leaving the detector without interacting are not taken into account because of the impossibility to measure their momentum. In Table 7 the results of this analysis are given for the different channels[a], normalised to an integrated intensity of 16×10^{19} *pot*.

The expected sensitivity for ICARUS (SUPER-I) on Δm^2, for full mixing and at the 90% C.L., is $1.1\times10^{-3}\ eV^2 (0.3\times10^{-3}\ eV^2)$. While, given an expected background

[a] r_m is defined as the ratio between the p_T and the scalar sum of transverse momenta (all with respect to the incoming neutrino direction) of the τ candidate, the recoiling jet and the missing momentum.

Cut	ν_τ eff.	ν_eCC	ν_τ evts. ($\Delta m^2 = 10^{-3}\ eV^2$)	ν_τ evts. ($\Delta m^2 = 5 \times 10^{-3}\ eV^2$)
electron				
Initial	1	2180	39.2	950
$E_{vis} < 17\ GeV$	0.772	218	30.2	487
$0.1 < p_T^e < 0.65\ GeV$	0.438	57	17.1	321
$p_T^{miss} > 0.75\ GeV$	0.227	5	8.9	192
$0.1 < \phi_{eh} < 0.7$	0.157	2.0 ± 0.2	6.2	170
hadron				
Initial	1	84375	110	2645
$M_T < 2\ GeV$	0.73	25763	80	1931
$p_T > 1.8\ GeV$	0.035	0.7 ± 0.3	4	96
ρ				
Initial	1	84375	110	2645
$M_T < 2\ GeV$	0.54	13352	60	1428
$p_T > 1.8\ GeV$	0.04	0.7 ± 0.3	4.4	105
three-pion				
Initial	1	84375	33	793
$0.6 < m_{3\pi} < 1.7\ GeV$	0.774	21778	26	614
$M_T < 2\ GeV$	0.69	10226	23	547
$r_m < 0.3$	0.527	3026	17	418
$p_T > 2.2\ GeV$	0.064	0.3 ± 0.2	2.1	50

Table 7. Summary of the electron, single hadron, exclusive ρ and three-pion channel analyses with the SUPER-I detector.

of 2.5 and 3.7 events for ICARUS and SUPER-I respectively, the discovery potential at 4σ at full mixing corresponds to $\Delta m^2 = 1.8 \times 10^{-3}\ eV^2$ and $\Delta m^2 = 0.9 \times 10^{-3}\ eV^2$.

9. The MINOS experiment at NuMI

A neutrino programme aimed at the study of neutrino oscillations was proposed since 1989 at Fermilab. The idea is to use the high intensity proton beam of the future Main Injector to provide an intense source of neutrinos. The neutrino beam has been already discussed in Section . Here we focus on the MINOS experiment [5] (Main Injector Neutrino Oscillation Search) which has been proposed (and approved) to search for neutrino oscillations in a long baseline configuration. MINOS and the NuMI beam have been optimised for a disappearance search in the oscillation parameter region corresponding to the Super-Kamiokande results. In the case of positive result, a follow up appearance search for $\nu_\mu \leftrightarrow \nu_\tau$ oscillations is envisaged.

Motivated by the requirements of a disappearance experiment, the MINOS detector is composed of a *near* detector located at the Fermilab site (290 m from the

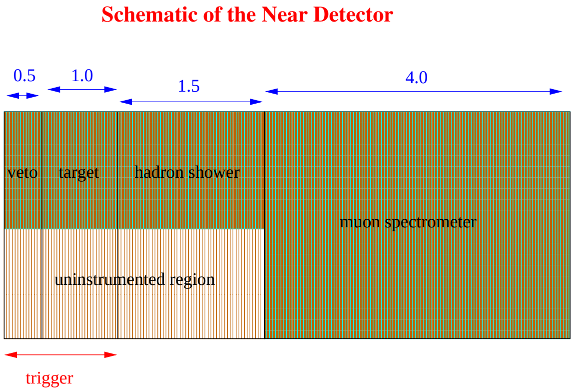

Fig. 14. Schematic view of the MINOS near detector.

neutrino source), and of a *far* detector in the Soudan mine in Minnesota, $\sim 730\ km$ away. In order to reduce systematic errors due to the knowledge of the beam flux, the near detector has a design similar to the far apparatus. Both detectors have the same absorber thickness, active elements, granularity, magnetic field and geometrical shape.

The total mass of the near detector is $\sim 1\ ton$. It consists of four parts, as shown in Fig. 14: a veto system which guarantees that there are no interactions induced by neutrons; a target, $1\ m$ thick iron, where neutrino interactions occur; a hadron catcher ($1.5\ m$ thick) which contains showers induced by neutrino interactions occurring in the target; a muon spectrometer allows to range out the muons and/or measure their momentum by curvature. It is made of iron plates ($2.54\ cm$ thick) interleaved with scintillator strips $1\ cm$ thick, $4.1\ cm$ wide and $8\ m$ long.

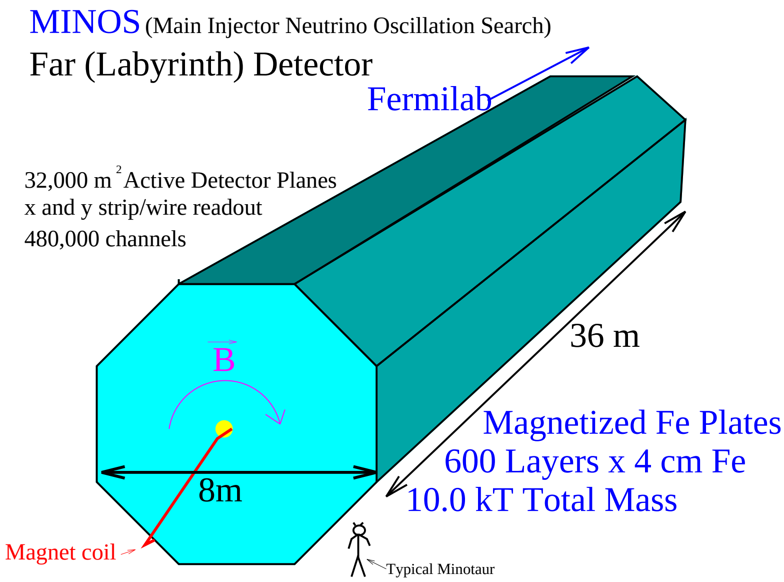

Fig. 15. The MINOS far detector.

Parameter	Value
Energy scale calibration	5% absolute, 2% near-far
EM energy resolution	$23\%/\sqrt{E(GeV)}$ ($< 5\%$ constant term)
Hadron energy resolution	$60\%/\sqrt{E(GeV)}$ ($< 7\%$ constant term)
Muon momentum resolution	$< 12\%$ (from curvature or range)
Neutral (NC) charged (CC) current event separation	Efficiency $> 90\%$ (99.5% with corrections)
Electron/π separation	Hadron rejection $\sim 10^3$ for $\varepsilon_e \sim 20\%$

Table 8. MINOS experimental parameters.

The far detector is a 5400 *ton* magnetised iron calorimeter with scintillator strips as active elements. The basic module is a 8 *m* diameter, 2.54 *cm* thick steel plane, followed by a 1 *cm* thick scintillator plane. Each scintillator plane is made up of 192 strips, each one 4 *cm* wide and up to 8 *m* long, depending on the actual position in the plane. The orientation of the strips is alternated by $\pm 90°$ in successive planes. A MINOS supermodule is made up of 242 such modules. Two supermodules compose the baseline MINOS far detector. The average magnetic field in the iron is 1.5 T. A schematic view of the far detector is shown in Fig. 15. The main features of MINOS are presented in Table 8.

The very good CC-NC event separation, together with the good energy resolution of the detector allow three different statistical approaches to detect neutrino oscillations: the near/far test, the NC/CC ratio measurement and the CC event energy measurement. Three beam design have been considered for the experimental programme. The expected results obtained using the high (PH2 high) and low (PH2 low) energy beams are shown in Fig. 16 and Fig. 17, respectively.

10. A calorimetric detector for the NGS: NOE

The NOE experiment [8)] has been proposed as a long baseline experiment in the NGS beam. The experiment is aimed at a search for $\nu_\mu \leftrightarrow \nu_\tau$ oscillations performed with a large scale transition radiation detector (TRD) and at a $\nu_\mu \leftrightarrow \nu_x$ search by means of a massive calorimeter (CAL). The calorimeter weights 5.6 *kton* and is based on the scintillating fibre technology. It is subdivided into modules interleaved with TRD detector planes, 2.4 *kton* in total.

A schematic view of the NOE detector is shown in Fig. 18. The energy resolution for electrons and hadrons has been evaluated to be $\sigma(E)/E = 17\%/\sqrt{E(GeV)} + 1\%$ and $\sigma(E)/E = 42\%/\sqrt{E(GeV)} + 8\%$, respectively. The muon direction and the hadronic shower axis are measured with an angular resolution $\sigma_\mu(\theta) = 1.27°\sqrt{E_\mu} + 2.27°/E_\mu$ and $\sigma_h(\theta) = 10°/\sqrt{E_h} + 20°/E_h$, respectively.

Combining both CAL and TRD information, the rejection power in separating electrons from minimum ionising particles is expected to be better than 10^{-3}. The

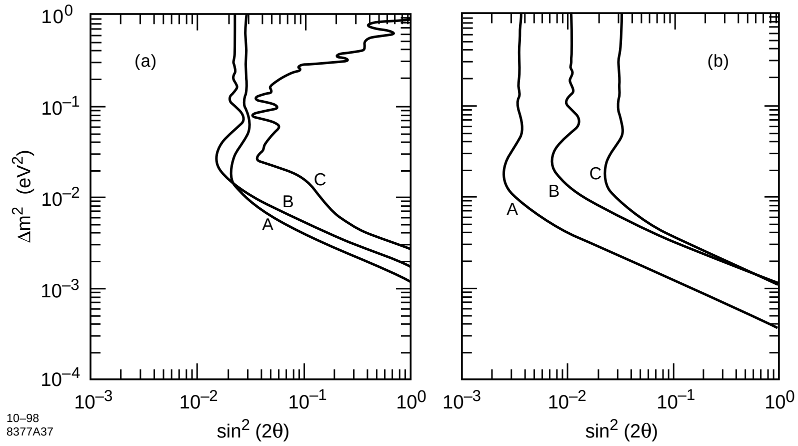

Fig. 16. 90% C.L. limits on neutrino oscillation parameters which would be established by MINOS with 10 $kton/yr$ in the absence of oscillations, using the PH2 (high) beam. The A, B and C curves show limits obtained from different oscillation tests. (a) $\nu_\mu \leftrightarrow \nu_\tau$ limits, where A refers to the near-far event rate comparison, B to the NC/CC ratio test and C to the CC-event energy test. (b) $\nu_\mu \leftrightarrow \nu_e$ limits, where the curve A stands for the electron appearance test, B for the NC/CC ratio and C for the near-far event rate comparison.

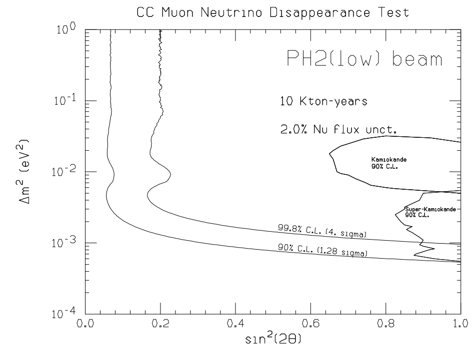

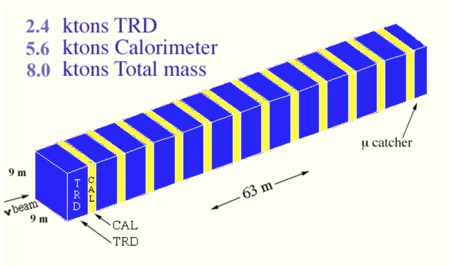

Fig. 17. (left) MINOS sensitivity for the ν_μ disappearance test (90% C.L. and 4σ contour) for a 10 $kton/yr$ exposure in the low energy PH2 (low) neutrino beam.

Fig. 18. (right) Schematic view of the NOE detector.

e/π^0 discrimination relies on the low density of the TRD material. In fact, γ's produced in π^0 decays cross many TRD layers with low conversion probability.

Due to the low background level and the good electron identification capabilities of the TRD, the $\nu_\mu \leftrightarrow \nu_\tau$ oscillation search is performed by exploiting the $\tau \to e$ channel. The identification of ν_τ CC interactions proceeds through a kinematical analysis similar to the one developed by NOMAD. Details about the analysis procedure and the detection efficiency can be found in [8]. The overall detection efficiency times branching ratio expected for the $\tau \to e$ channel is $\sim 3.5\%$, against a rejection power of about 70 for ν_e CC events and $\sim 10^3$ for ν_μ NC events.

A search for $\nu_\mu \leftrightarrow \nu_\tau$ oscillations based on the NC/CC method can also be performed by using a low energy version of the NGS beam. The sensitivity reachable by this search is comparable to the one of the appearance method, provided the availability of a near detector.

11. The AQUA-RICH experiment

The proposed AQUA-RICH [9] experiment exploits the water Cerenkov technique to measure the kinematical quantities for particles produced in neutrino interactions. It has been demonstrated [27] that it is possible to determine momentum, direction and velocity of hadrons and muons from width, position of centre and radius of Cerenkov rings, respectively. Momentum is measured if multiple scattering is the main cause of the ring width. Monte Carlo simulations showed that hadrons can be detected up to 9 GeV with $\sigma_p/p < 7\%$ and muons up to 40 GeV with $\sigma_p/p < 2\%$. The track direction is determined from the ring image with an error $\sigma_\theta \leq 5$ mrad. The track reconstruction (photon emission point) requires a timing resolution $\sigma_t < 1\ ns$.

The AQUA-RICH detector consists of 125 $kton$ of water [9]. It is aimed at a search for $\nu_\mu \leftrightarrow \nu_\tau$ oscillations in appearance mode in the NGS beam and at the detection of atmospheric neutrinos. Regardless of the neutrino source, the analysis is performed by fully reconstructing the kinematics of final state charged particles, hence constraining the initial neutrino energy.

Signal and background Monte Carlo events, generated by assuming a relatively low energy neutrino beam, have been used to study the AQUA-RICH capability in searching for $\nu_\mu \leftrightarrow \nu_\tau$ oscillations with a LBL experiment (Fig. 19).

The τ signal could be observed by selecting quasi elastic events $\nu_\tau n \to \tau p$, followed by a muonic decay, with both the muon and the proton above threshold. A good separation between ν_τ signal and ν_μ background can be achieved. The experiment is expected to reach a sensitivity to Δm^2 of about of $1 \times 10^{-3}\ eV^2$ at full mixing.

12. Conclusions and outlook

As an exercise, we can compare sensitivities and discovery potential of the pro-

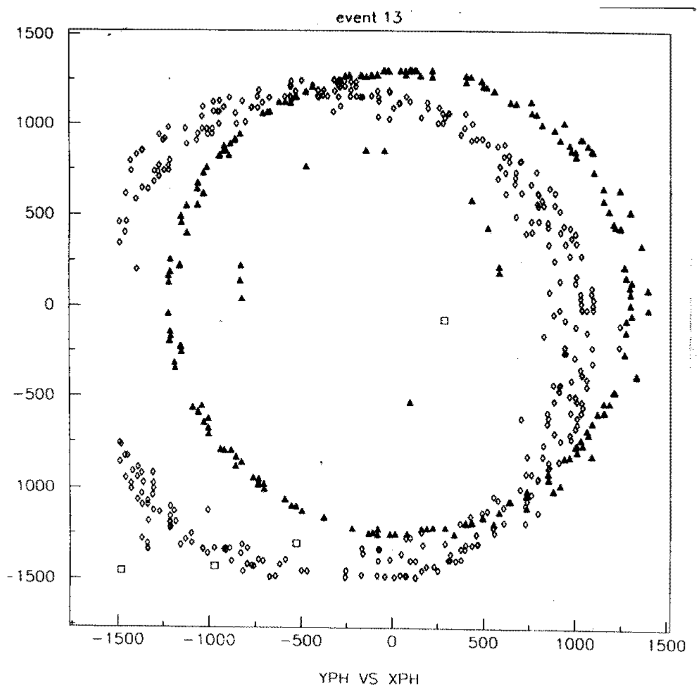

Fig. 19. Simulation of an AQUA-RICH quasi-elastic event $\nu_e p \rightarrow e^- \Delta$ and $\Delta \rightarrow p\,\pi^+$ for $E_\nu = 12\ GeV$. It shows two proton rings (black triangles) and one electron ring (open diamonds). There is also a hint for a pion ring (open squares).

posed NGS LBL experiments for $\nu_\mu \leftrightarrow \nu_\tau$ oscillations, which exploit the appearance technique. We have assumed the NGS performance indicated by the SPSC/LNGSC committees in their call for LoI in 1998 [29]. The typical sensitivity which could be reached in the absence of oscillations is similar for all the experiments. The minimum Δm^2 (Δm^2_{min}) at full mixing excluded at 90% C.L. for the various experiments is reported in Table 9.

The number of detected τ events as a function of Δm^2, at full mixing, is listed in Table 10. The discovery potential of all experiments (Table 9) extends well below the Super-Kamiokande best fit point ($\Delta m^2 = 3.5 \times 10^{-3}\ eV^2$ and $\sin^2 2\theta = 1$).

The above considerations indicate that the future NGS/Gran Sasso programme has large potentialities for τ appearance searches, relevant for the clarification of the atmospheric neutrino anomaly. If one also includes the K2K and NuMI facilities, it becomes clear that the predictable future of LBL neutrino oscillation searches will be very exciting.

Several scenarios can be depicted. By the year 2000 K2K could confirm the disappearance of muon neutrinos within a large part of the parameter domain allowed by the Super-Kamiokande result. The MINOS experiment will then measure with higher sensitivity the disappearance probability and hopefully perform an appearance search. Dedicated direct-appearance experiments at Gran Sasso could prove the

Experiment	Back.	Δm^2_{min} (eV^2) Sensitivity	Δm^2_{min} (eV^2) Discovery
ICARUS	2.5	1.1×10^{-3}	1.8×10^{-3}
SUPER-I	3.7	0.3×10^{-3}	0.9×10^{-3}
OPERA	0.41	1.1×10^{-3}	1.8×10^{-3}
NOE	3.7	2.2×10^{-3}	4.7×10^{-3}
AQUARICH	< 1	1.4×10^{-3}	2.3×10^{-3}

Table 9. Expected background and minimum Δm^2 (full mixing) of appearance experiments proposed for the NGS.

Experiment$\backslash\Delta m^2_{min}$ (eV^2)	2×10^{-3}	3.5×10^{-3}	5×10^{-3}
ICARUS	13	40	85
SUPER-I	70	200	420
OPERA	6	20	40
NOE	2	7	15
AQUARICH	10	30	60

Table 10. Detected τ events as a function of Δm^2 at full mixing.

existence of $\nu_\mu \leftrightarrow \nu_\tau$ oscillations by finding a handful of tau's, even down to small Δm^2 values.

However, even more complicated solutions could be verified, profiting of the existence of a global worldwide programme, based on the availability of several beam facilities and of experiments employing different detection techniques and methods. In five-ten years from now the source of the atmospheric neutrino deficit could be known, hence opening the season of the next-generation, high-precision measurements.

13. Acknowledgements

A.E. wishes to warmly thank Milla and the Organizing Committee for the perfect organisation of the Workshop and for the pleasant and stimulating atmosphere.

14. References

1) Y. Fukuda et al., *Phys. Rev. Lett.* **81** (1998) 1562.
2) Y. Fukuda et al., *Phys. Lett.* **B335** (1994) 237.
3) M. Apollonio et al., *Phys. Lett.* **B420** (1998) 397.
4) K. Nishikawa et al., KEK Report **E362** (1995); Y. Oyama (K2K Coll.), Proc. of the YITP Workshop on Flavor Physics, Kyoto, 1998 (hep-ex/9803014).
5) E. Ables et al., Fermilab Proposal P-875 (1995); NuMI-L-337 (1998); NuMI-L-375 (1998);
http://www.hep.anl.gov/NDK/Hypertext/numi.html.

6) The Fermilab NuMI Group, Fermilab Report NuMI-346, October 1998.
7) ICARUS Proposal, LNGS-94/99-I (1994); J.P. Revol et al., ICARUS-TM-97/01; ICARUS Collaboration CERN/SPSC-98-33.
8) M. Ambrosio et al. (NOE Coll.), *Nucl. Instr. and Meth.* **A363** (1995) 604; CERN/SPSC-98-32.
9) P. Antonioli et al., CERN/SPSC-98-37; http://pclvd2.bo.infn.it/rich/aqr6.ps
10) A. Ereditato, K. Niwa and P. Strolin, INFN/AE-97/06 and Nagoya DPNU-97-07, 27 January 1997; H. Shibuya et al., CERN/SPSC-97-24; K. Kodama et al., CERN/SPSC-98-25.
11) M. Apollonio et al., CERN/SPSC-98-34.
12) G. Acquistapace et al., CERN 98-02, INFN/AE-98/05, 19 May 1998.
13) G.J. Feldman and R.D. Cousins, *Phys. Rev.* **D57** (1998) 3873.
14) E. Heijne, CERN Yellow Report 83-06, 1983; G. Acquistapace et al., CERN Preprint, CERN-ECP/95-14, 1995.
15) A. Ereditato et al., ICARUS-TM-98/13, OPERA 980722-01.
16) NGS: addendum to the design (note in preparation).
17) E. Eskut et al., Nucl. Instr. and Meth. A 401 (1997) 7; E. Eskut et al., *Nucl. Instr. and Meth.* **A401** (1998) 7.
18) S. Aoki et al., *Nucl. Instr. and Meth.* **B51** (1990) 446; T. Nakano, Ph.D. Thesis, University of Nagoya (1997).
19) A. Ereditato, G. Romano and P. Strolin, CERN-PPE/96-106, *Nucl. Phys.* **B54** (1997) 139.
20) A. Ayan et al. (TOSCA Coll.), CERN-SPSC/97-5; A. Ayan et al. (TOSCA Coll.), CERN-SPSC/98-20.
21) K. Niwa, in "Physics and Astrophysics of Neutrinos" editors M. Fukugita and A. Suzuki, Springer-Verlag, (1994) 520.
22) J. Nishimura, Handbuch der Physik, Springer-Verlag, Vol. 46/2 (1967) 1.
23) Y. Fujimoto and S. Hayakawa, Handbuch der Physik, Springer-Verlag, Vol. 46/2 (1967) 115.
24) S.G. Bayburina et al., *Nucl. Phys.* **B191** (1981) 1.
25) ICARUS Coll., CERN/SPSC-98-33, SPSC/M620.
26) NOMAD Coll., P. Astier et al., CERN-SPSLC/91-21 (1991), CERN SPSLC/9148, SPSLC/P261 Add.1.
27) T. Ypsilantis et al., CERN-LAA/96-13, 1996.
28) A. Habig (Super-Kamiokande Coll.), Talk given at the American Physical Society Division of Particles and Fields, UCLA Los Angeles, 1999; hep-ex/9903047.
29) Joint SPSC-LNGSC meeting held at CERN on November 3-4, 1998.